Journal of Hazardous Materials 499 (2025) 140221

Contents lists available at ScienceDirect

Journal of Hazardous Materials

journal homepage: www.elsevier.com/locate/jhazmat

Partitioning dynamics of polycyclic aromatic hydrocarbons and their derivatives in water-sediment systems: Implications for microbial community perturbations and enhanced anthropogenic pathogenicity in riverine ecosystems

Chao Wang [a,b], Jialin Shi [a,b], Jiana Zhao [a,b], Yi Zhong [a,b], Fan Wang [a,b], Jukun Xiong [a,b], Wanjun Wang [a,b,*]

[a] Guangdong Key Laboratory of Environmental Catalysis and Health Risk Control, Guangdong Hong Kong-Macao Joint Laboratory for Contaminants Exposure and Health, Institute of Environmental Health and Pollution Control, Guangdong University of Technology, Guangzhou 510006, China
[b] Guangzhou Key Laboratory Environmental Catalysis and Pollution Control, Guangdong Basic Research Center of Excellence for Ecological Security and Green Development, School of Environmental Science and Engineering, Guangdong University of Technology, Guangzhou 510006, China

HIGHLIGHTS

- SPAHs preferentially persist in water phase, while PPAHs dominated in sediment phase.
- Hydrophilicity of substituent group in SPAHs determined their partitioning behaviors.
- PPAHs/SPAHs partitioning drove phase-specific microbial responses and shaped keystone species.
- SPAHs pressure induced anthropogenic pathogenicity amplification in water phase.

GRAPHICAL ABSTRACT

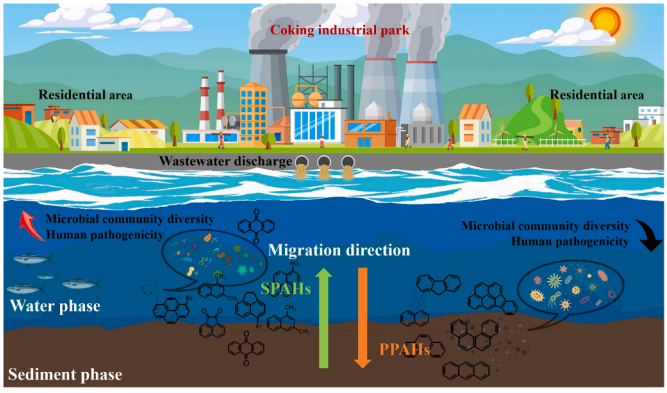

ARTICLE INFO

Keywords:
Substituted polycyclic aromatic hydrocarbons
Partitioning dynamics
Water-sediment system
River microbiome
Anthropogenic pathogenicity

ABSTRACT

Polycyclic aromatic hydrocarbons (PAHs) and their derivatives have posed impressive threats to riverine ecosystems. However, their partitioning dynamics in water-sediment systems and consequent impacts on river microbiome remain unexplored. This study investigated the distribution profiles, partitioning behaviors, and microbial responses of 18 parent PAHs (PPAHs) and 68 substituted PAHs (SPAHs) in water-sediment systems in Baishinan River, which receives wastewater effluents from a typical coking industrial park in Taiyuan City, Shanxi Province, China. SPAHs dominated water phase (81.6 % ΣPAHs), while PPAHs prevailed in sediment phase (72.5 % ΣPAHs). Fugacity model further revealed that hydrophilic SPAHs (e.g., oxygenated-PAHs and nitro-PAHs) exhibited water-phase enrichment, whereas hydrophobic PPAHs underwent sedimentary

* Corresponding author at: Guangdong Key Laboratory of Environmental Catalysis and Health Risk Control, Guangdong Hong Kong-Macao Joint Laboratory for Contaminants Exposure and Health, Institute of Environmental Health and Pollution Control, Guangdong University of Technology, Guangzhou 510006, China.
E-mail address: wanjun@gdut.edu.cn (W. Wang).

https://doi.org/10.1016/j.jhazmat.2025.140221
Received 14 July 2025; Received in revised form 19 September 2025; Accepted 21 October 2025
Available online 24 October 2025

sequestration. High-throughput sequencing demonstrated that SPAHs triggered water-phase microbial functional specialization, elevating α-diversity (+16 %), PAH degradation (*bphA* +85.8-fold), and virulence factor genes (*mecA* +69-fold). Conversely, PPAHs reduced the α-diversity and inhibited metabolic pathways in benthic microbiota. Notably, SPAHs stimulated the proliferation of human pathogens (*Burkholderia*, *Burkholderiales*, and *Corynebacterium*) and amplified the abundance of genes associated with human disease. Structural equation modeling confirmed SPAHs as the primary driver of pathogenicity, highlighting the enhanced pathogenic risks in riverine ecosystems due to industrial PAH emissions. This work establishes a mechanistic framework for understanding contaminant phase partitioning-mediated microbial function shifts, offering critical insights for environmental risk mitigation and public health protection.

1. Introduction

With the advancement of human socio-economic development, industrial pollutant emissions pose escalating threats to aquatic ecosystems [9]. Polycyclic aromatic hydrocarbons (PAHs), characterized by persistence, mutagenicity, teratogenicity, and carcinogenicity, exhibit ubiquitous occurrence and have been extensively detected in diverse aquatic environments, including rivers, lakes, and marine systems [34,47]. Human activities govern not only the discharge and concentration of PAHs but also their subsequent distribution between water and sediment [21,59]. Global regulatory attention has prioritized PAH contamination, exemplified by the U.S. Environmental Protection Agency's designation of 16 parent PAHs (PPAHs) as priority pollutants. Upon entering aquatic environments, the PPAHs would undergo various chemical and biological reactions mediated by hydrolysis, photolysis, and microbial degradation, to become PAH derivatives also called substituted PAHs (SPAHs). These SPAHs typically include methyl-PAHs (MPAHs), nitro-PAHs (NPAHs), oxygenated-PAHs (OPAHs), chlorinated-PAHs (ClPAHs), brominated-PAHs (BrPAHs), and heterocyclic-PAHs (HPAHs) [26]. Notably, SPAHs have been demonstrated to show enhanced toxicity compared to PPAHs [41]. For example, the carcinogenicity of 6-nitro-Chrysene to humans is 10 times that of Benzo[*a*]pyrene [58]. Thus, underscoring the imperative to evaluate the ecological impacts of both PPAHs and SPAHs.

In aquatic ecosystems, microorganisms play pivotal roles in organic matter degradation, nutrient cycling, pollutant transformation, and trophic network maintenance [45,63]. Perturbations in microbial ecology may trigger cascading environmental consequences, including eutrophication, toxicant bioaccumulation, biodiversity erosion, and pathogenic microorganism proliferation, ultimately jeopardizing ecosystem integrity and human health [43,5,54]. Consequently, elucidating the ecological ramifications of PPAHs and SPAHs inputs on aquatic microbial communities represents a critical research frontier for environmental sustainability and public health protection.

Industrial activities such as coking, petrochemical and smelting, have discharged huge amounts of PAHs and their derivatives into receiving rivers. The ecological impacts of PAHs in receiving rivers are intrinsically linked to their partitioning dynamics between water and sediment phases [15]. Typically, the partitioning behavior of PAHs in water-sediment systems is governed by their sources and environmental factors, including wastewater discharge, atmospheric deposition, hydrodynamic conditions, and sediment properties. In addition, physicochemical characteristics of PAHs, such as polarity, octanol-water partition coefficient (K_{ow}), molecular weight, and molecular structures, significantly modulate their interphase distribution [13,32]. Previous studies have demonstrated that low-molecular-weight (LMW) PPAHs (3–4 benzene rings) predominantly present in the water phase, whereas high-molecular-weight (HMW) PPAHs (5–6 benzene rings) exhibited preferential adsorption onto sediment matrices [6], attributable to their heightened hydrophobicity. However, limited studies exist regarding the partitioning mechanisms of SPAHs across water-sediment interfaces. Liu et al. [28] investigated the partitioning behaviors of diverse PAHs in the Black River's sediment-porewater system, revealing that the distribution of SPAHs (e.g., NPAHs and OPAHs) between phases correlates critically with substituent group characteristics, thereby distinguishing their partitioning patterns from those of PPAHs. Nevertheless, under industrial pollution scenarios, the dynamic distribution patterns of both PPAHs and SPAHs in receiving rivers, as well as their distinct transport mechanisms and partitioning behaviors, remain inadequately resolved.

Meanwhile, microbial community composition, metabolic processes, and enzyme activities are highly sensitive to exogenous contaminants. For instance, Lu et al. [33] demonstrated that high-concentration PPAH inputs in natural bay systems reduced sediment-phase microbial diversity while concurrently enriching PPAH-degrading bacterial taxa, indicating that PPAHs exposure significantly restructured microbial communities and stimulated proliferative adaptation of degradative consortia. Liu et al. [30] investigated microbial functional shifts in urban river sediment microbiomes under PPAH contamination, revealing that elevated PPAH concentrations decreased community diversity and identified *Spirochaetia*, *Aminicenantia*, and *Deltaproteobacteria* as keystone taxa, which are responsible for the metabolism of PPAHs. Comparative analyses by Lin et al. [24] on water-phase microbial community assembly under PPAHs pollution demonstrated a predominance of deterministic processes in highly PPAH-contaminated waters versus stochastic processes dominated in low PPAH-contaminated areas, indicating that the pollution level of PPAHs changes the assembly process of microbial community. Recently, some reports have also pointed out that the environmental stress from contaminant inputs increased the risk of pathogenicity transmission by re-shaping the microbial community. For instance, Liu et al. [31] have found that multi-contaminant stressors (heavy metals, pesticides, microplastics, and antibiotic resistance genes) triggered microbial genomic adaptations enhancing stress resilience, yet concomitantly upregulated pathogenic gene expression. Wang et al., [49] have reported that the environmental stress from PPAHs significantly amplified coastal microbial resistomes, significantly elevating the abundances of antibiotic resistance genes (ARGs; e.g., *sul1*, *aadA2*) and integron-associated genes (*intI1*), resulting in enhanced horizontal gene transfer and dissemination of anthropogenic pathogenicity. Nevertheless, the mechanistic linkages among SPAH stress, microbial community assembly, and pathogenicity dissemination remain unexplored. Particularly within industrially impacted riverine sediment-water systems, the partitioning dynamics of PPAHs/SPAHs and their differential impacts on microbial community structure and anthropogenic pathogenicity evolution have not been systematically studied.

Coking industry has been recognized as one of the major pollution sources for PAH emissions through wastewater discharges [55]. Therefore, a receiving river adjacent to a typical coking industrial park was targeted to investigate the partitioning dynamics of 86 PAHs (including 18 PPAHs and 68 SPAHs) in water-sediment systems and their impacts on riverine microbiomes. The aims of this study were: (1) to characterize the occurrence patterns and ecological risks of PPAHs and SPAHs in water and sediment phases of the coking-impacted receiving rivers; (2) to decipher the partitioning behaviors and mechanisms governing PPAHs and SPAHs distribution in the water-sediment systems, (3) to reveal differential impacts of PPAHs/SPAHs inputs on microbial community structures in water and sediment, and identify key functional taxa and their microbial function changes under the stress of PAHs, and

(4) to unravel the effects of PPAHs/SPAHs inputs on the regulation of microbial community assembly and pathogenicity propagation. This study pioneers the systematic investigation into how divergent partitioning behaviors of PPAHs and SPAHs modulate microbial community assembly in water-sediment system, uncovering their critical roles in disseminating microbial pathogenicity.

2. Materials and methods

2.1. Chemicals and reagents

Chemicals and reagents used in this study are described in Text S1. Additional information about the targeted 86 PAH standards is listed in Table S1.

2.2. Field site description and sampling

Field sampling campaign was conducted in November 2021 along Baishinan River, which receives wastewater effluents from a typical coking industrial park located in Taiyuan City, Shanxi Province, China (112°10'—112°22'E, 37°30'—37°35'N). Sampling sites were located in the upstream (SX1–SX5), midstream (SX6—SX10), and downstream (SX11–SX13) of the Baishinan River (Table S2). Sampling points were distributed non-uniformly to reflect the varying environmental heterogeneity across different river reaches, with a higher density in the more complex upstream and midstream areas. As shown in Fig. 1(a), upstream sampling sites were situated near human settlements without industrial impacts, whereas midstream sites encompassed the coking wastewater effluent discharge zone, and downstream sites were located in residential areas without industrial effluent inputs. The coking plant has been operating steadily for 15 years. According to the field survey, there is a

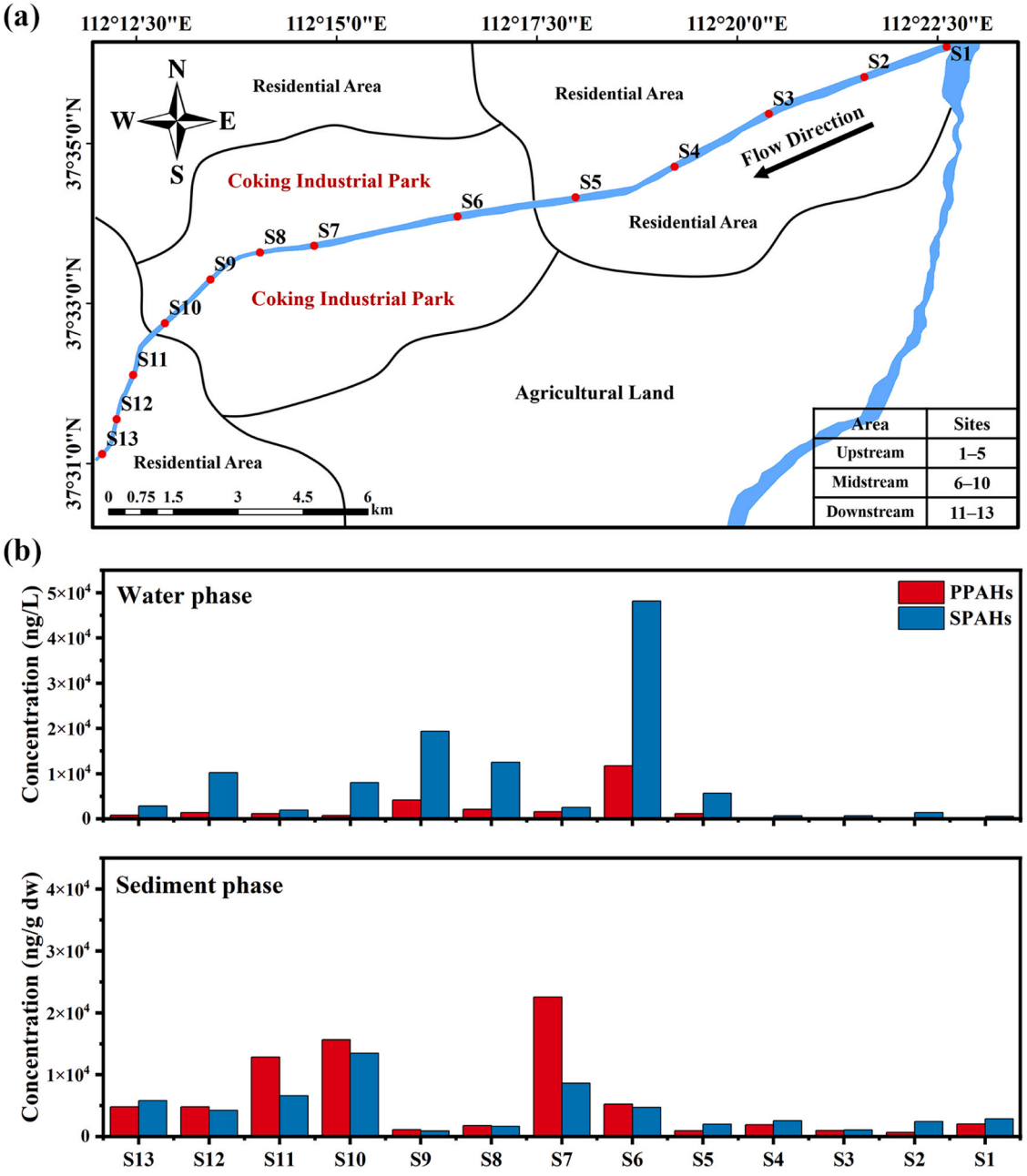

Fig. 1. (a) Description of sampling sites in the study area; (b) total concentrations of parent PAHs (PPAHs) and substituted PAHs (SPAHs) in water and sediment phase of the receiving river.

large number of trucks transporting coal all year round, and the local heating system is currently in operation. Therefore, besides industrial pollution, vehicle exhaust pollution and coal burning may also occur in this area.

Water and sediment samples were collected following established protocols [10,50]. Surface water (0.4–0.6 m depth) was collected in triplicate using 1 L amber glass bottles, acidified with sulfuric acid to suppress microbial activity, and stored at 4°C for PAH analysis. For microbial enrichment, 1 L of surface water was filtered through a 0.22 μm cellulose acetate membrane (Millipore, 47 mm), which was subsequently sealed in sterile plastic bags, flash-frozen in liquid nitrogen, and maintained at −80°C until processing. Sediment samples were collected in triplicate at each site using a 5 L aluminum grab sampler (Taitian Instruments Co. Ltd., Guangzhou). Homogenized subsamples (500 g) were preserved at −18°C for PAH quantification, while 100 g samples were flash-frozen and stored at −80°C for microbial analysis. Detailed sampling procedures are provided in Text S2.

2.3. Sample pretreatment and instrumental analysis

PAHs in water phase were extracted from water samples using liquid-liquid extraction, while the PAHs in sediment phase were extracted from sediment samples using accelerated solvent extraction [48]. After standard pre-concentration and purification procedures, PAHs were analyzed using a gas chromatograph coupled to a mass spectrometer (7890B-7000C, Agilent, USA). Detailed analysis methods, quality assurance and quality control procedures, and results of water and sediment environmental factors can be found in Text S3–S4 and Table S3–S4.

2.4. Water-sediment partition of PPAHs and SPAHs

Fugacity model was used to study the partitioning behaviors of PPAHs and SPAHs in water-sediment system. The fugacity fraction (*ff*) of PPAHs and SPAHs between water and sediment was calculated by Eqs. (1–2) [25]:

$$ff = \frac{K'_{OC}}{K'_{OC} + K_{OC}} \quad (1)$$

$$K'_{OC} = \frac{C_s}{C_w \times f_{OC}} \quad (2)$$

where K_{oc} (L/g) is the organic carbon normalized partitioning coefficients of PAHs; K'_{oc} (L/g) is the sediment-water partitioning coefficient; C_s (ng/g dw) is the concentration of PAHs in sediments; C_w (ng/L) is the concentration of PAHs in water phase; f_{OC} is the organic carbon fraction of the sediments (%), which are listed in Table S3. When $ff < 0.3$, it indicates a net flux from water to sediments, which acts as a sink for PAHs. When $0.3 < ff < 0.7$, PAHs are in water-sediment equilibrium. When $ff > 0.7$, it shows a net flux from sediments into water, where sediments act as a secondary emission source of PAHs [16].

2.5. DNA extraction and 16S rRNA gene amplicon sequencing

Bacterial genomic DNA was extracted from water and sediment with Rapid Soil DNA Isolation Kit (Sangon, China) and purified with Ezup Column Bacteria Genomic DNA Purification Kit (Sangon, China) [51]. DNA integrity and purity were assessed via UV-Vis spectrophotometry (NanoDrop 2000, Thermo Scientific, USA). The hypervariable V3–V4 region of the bacterial 16S rRNA gene was amplified using primer pairs 338 F (5'-ACTCCTACGGGAGGCAGCAG-3') and 806 R (5'-GGACTACHVGGGTWTCTAAT-3') under optimized PCR conditions. Detailed PCR protocols and steps on bioinformatic analysis are listed in Text S5. Sequencing data that support the findings of this study are available at the NCBI Sequence Read Archive (project accession number PRJNA1280091).

2.6. Ecological risk assessment and source apportionment

Ecological risks of PAHs to aquatic organisms in the receiving river were evaluated through risk quotient (RQ) analysis (Text S6). The acute and chronic toxicity parameters used in this model are listed in Table S5. Source apportionment of PAHs was conducted using the positive matrix factorization (PMF) model, and the details can be found in Text S7.

2.7. Statistical Analysis

Spatial distribution patterns of PAHs were visualized using ArcGIS 10.8 (ESRI Inc., Redlands, CA), with statistical graphics generated in OriginPro 2024 (OriginLab Corporation, USA). Microbial α-diversity was analyzed through Chao1, ACE, and Shannon indices, representing community richness and diversity metrics. β-diversity patterns across sample groups were evaluated via Analysis of Similarities (ANOSIM) and non-metric multidimensional scaling (NMDS) ordination based on Bray-Curtis dissimilarity matrices, with inter-group significance determined by Kruskal-Wallis tests. Spearman correlation was used to analyze the correlation between PAH concentrations (PPAHs/SPAHs), physicochemical properties, and microbial composition. Co-occurrence network analysis with Zi-Pi topological features identified keystone species and module hubs within bacterial consortia. Functional profiles were inferred using PICRUSt2 with Kyoto Encyclopedia of Genes and Genomes (KEGG) Orthology annotations to reveal the PAH-induced metabolic perturbations.

3. Results and discussion

3.1. Occurrence of PPAHs/SPAHs in water-sediment system of the receiving river

In water phase, a total of 86 PAHs were monitored, and 72 of them were detected, including 18 PPAHs and 54 SPAHs at levels above the quantification limit. Total PAH concentrations (ΣPAHs) ranged from 790.3 to 59,826.8 ng/L (mean: 10,798 ng/L), exhibiting pronounced spatial heterogeneity with midstream concentrations (sites S6–S10) exceeding upstream (S1–S5) and downstream (S11–S13) levels by 9.9- and 3.6-fold, respectively (Fig. S1(a)). The spatial distribution also showed that the pollution was mainly concentrated in the outfall area in the middle reaches of the river (Fig. 1(b), Fig. S2(a)), confirming that the effluents discharged from the coking park had significantly polluted the midstream of the receiving river. Compared with other PAH-contaminated surface water systems worldwide, the ΣPAHs contamination in the midstream area of this study was at a high level of contamination (Table S6–S7). In sediment phase, 72 PAHs were detected with ΣPAHs ranging from 1579.9 to 28,146.9 ng/g dw (mean: 8440.8 ng/g dw). Similar to the results in water phase, ΣPAHs in sediment phase were also higher in the midstream area than that of the upstream and downstream areas (Fig. 1(b), Fig. S1(b), Fig. S2(b)). Notably, the concentrations of PAHs at S8 and S9 were relatively low. This is closely related to the hydrodynamic conditions at these river bend locations. The high flow velocity in this area may result in PAHs being difficult to settle [22]. Additionally, the lower TOC content in S8 and S9 (2.1 % and 0.9 %, respectively) also leads to a lower enrichment effect on PAHs compared to S10 (4.7 %) and S11 (12.5 %) [27]. Moreover, the discharge outlet is located upstream of S6, resulting in the highest concentration of water-phase PAHs at S6. However, sediment PAH concentrations peaked at S7. This is because the migration of PAHs from the water phase to the sediment phase at S6 is a prolonged process. Furthermore, sediment TOC content at S7 (7.9 %) was significantly higher than at S6 (3.6 %), indicating that sediments at S7 are more readily adsorbed and accumulate PAHs. PMF model was used for the identification and quantification of various sources of PAHs in water and

sediment phases. Fig. S3 illustrates the five sources of PAHs and the relative contributions in water and sediment phases. The water phase contains five sources (Fig. S3(a)), including secondary formation (10.2 %), coking oven emissions (49 %), traffic emissions (16.4 %), coal burning (18.8 %), and biomass burning (5.6 %). Additionally, four sources were identified in the sediment phase, including secondary formation (9.6 %), coking oven emissions (48 %), biomass burning and traffic emissions (32.5 %), and coal burning (9.9 %) (Fig. S3(b)). These results indicated that the pollution of PAHs in both water and sediment phases of this river mainly originated from the coking industry activities. The threat of PAHs to aquatic organisms (algae, invertebrates, and fish) was assessed based on toxicity parameters provided by the Ecological Structure Activity Relationships Predictive Model. Results showed that the acute risk (RQ_A) and chronic risk (RQ_C) of PAHs in the midstream of water phase were higher than those in the upstream and downstream areas by factors of 3.6–11.5 (Fig. S4, Table S8). In particular, 87.2 % of the RQ values in sediment phase exceeded the risk threshold (RQ >1), while the exceeding rate in water phase was only 50.0 %, demonstrating more substantial benthic ecotoxicological hazards linked to the coking industrial discharges.

The ΣPAHs in water phase were composed of 18.4 % PPAHs and 81.6 % SPAHs, suggesting SPAHs were the predominant form of PAHs in water phase (Fig. S5(a)). This may be attributed to the higher polarity of SPAHs compared to PPAHs, resulting in their greater hydrophilicity and easier presence in water phase [29]. OPAHs accounted for the largest composition of SPAHs in water phase with a relative contribution of 58.8 %. It was also the largest contributor to ΣPAHs (48.0 %). Among the OPAHs, 9,10-Phenanthrenequinone (9,10-PheQ) had the highest relative contribution (73 %, Fig. S5(b)), with an average concentration of 4263.4 ng/L. However, 9,10-PheQ has been neglected in other studies of OPAHs contamination in surface water [17]. This study indicated that 9,10-PheQ may be the characteristic SPAHs discharged by the coking industry. The coking process directly generates 9,10-PheQ through coal pyrolysis [23], which is then discharged via wastewater. Additionally, phenanthrene in water is transformed into 9,10-PheQ through photochemical and microbial processes [42]. This dual-source mechanism ensures its continuous presence. 9,10-PheQ is highly persistent due to its resistance to photolysis and slow microbial degradation [38], causing it to accumulate rather than break down. This persistence makes it a stable, cumulative marker of pollution, accurately tracing its spatial and temporal distribution. Different from the results in water phase, the ΣPAHs in sediment phase was composed of 72.5 % PPAHs and 27.5 % SPAHs (Fig. S5(c)), indicating that the sediment phase was dominated by PPAHs. The top three PPAHs in relative proportion were Fla (12.5 %), B[*b*]F (10.5 %), and Phe (8.9 %) (Fig. S5(d)). Mean concentrations of these PPAHs in the receiving river sediments (Fla: 764.3 ng/g dw; B[*b*]F: 640.9 ng/g dw; Phe: 547.7 ng/g dw) surpassed Chinese lacustrine sediment baselines by 24.6-, 16.0-, and 7.9-fold, respectively [12], suggesting their utility as diagnostic tracers for PPAH contamination in coking-impacted sediment systems. These results indicate significant differences in transport behaviors of PPAHs/SPAHs after their inputs into the receiving river: SPAHs preferentially persist in water phase, while PPAHs are inclined to accumulate in sediment phase. The differential environmental behavior underscores the necessity for phase-specific risk management strategies in industrial riverine ecosystems.

3.2. *Partitioning behavior and mechanisms of PPAHs/SPAHs in water-sediment systems*

To understand the different partitioning dynamics of PPAHs and SPAHs in aquatic ecosystems, the fugacity model was employed to assess

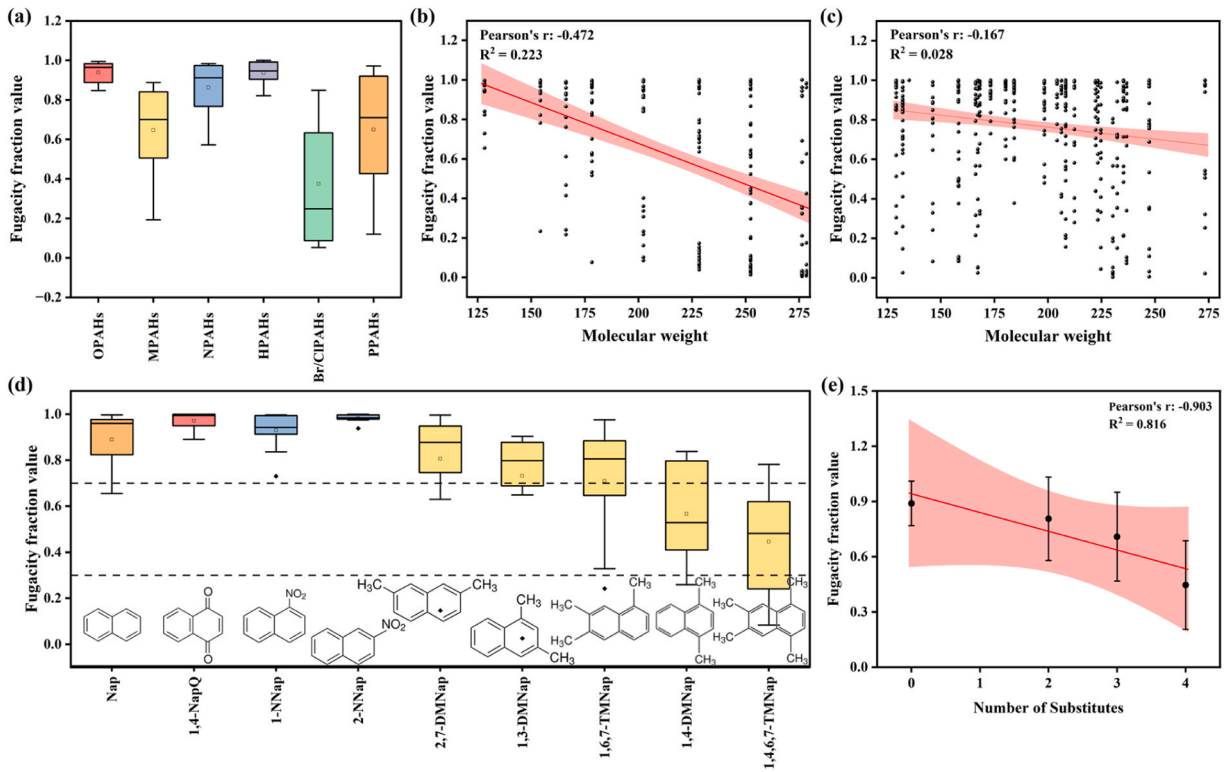

Fig. 2. (a) Fugacity fraction (*ff*) values of PPAHs and SPAHs (OPAHs: oxygenated-PAHs, MPAHs: methyl-PAHs, NPAHs: nitro-PAHs, HPAHs: heterocyclic-PAHs, Br/ClPAHs: chlorinated-PAHs and brominated-PAHs); Pearson correlation between molecular weight and *ff* values of (b) PPAHs and (c) SPAHs; (d) comparison of the *ff* values of naphthalene (Nap) and substituted Nap (1,4-NapQ: 1,4-Naphthoquinone, 1-NNap: 1-Nitronaphthalene, 2-NNap: 2-Nitronaphthalene, 2,7-DMNap: 2,7-Dimethylnaphthalene, 1,3-DMNap: 1,3-Dimethylnaphthalene, 1,6,7-TMNap: 1,6,7-Trimethylnaphthalene, 1,4-DMNap: 1,4-Dimethylnaphthalene, 1,4,6,7-TMNap: 1,4,6,7-Tetramethylnaphthalene); (e) Pearson correlation between methyl substituent number and *ff* values of methyl-substituted Nap. The lines in (b), (c), and (e) represent the linear regression model, and the shaded area represents the 95 % confidence interval.

and evaluate the partitioning of PPAHs and SPAHs between water and sediment (Table S9). Overall, the *ff* values of SPAHs, including OPAHs (ff_{mean} = 0.94), NPAHs (ff_{mean} = 0.86), and HPAHs (ff_{mean} = 0.94), was higher than that of PPAHs (ff_{mean} = 0.65) (Fig. 2(a)). Among them, there were 33 SPAHs (78.6 %) with ff_{mean} higher than 0.7, while there were only 9 PPAHs (50.0 %) with ff_{mean} higher than 0.7, indicating that SPAHs are more inclined to partition into the water phase. On the contrary, 16.7 % of PPAHs had a ff_{mean} of less than 0.3, compared to only 9.5 % of SPAHs, suggesting that PPAHs are more inclined to enter sediment phase during transportation.

Correlation analysis showed that molecular weight was negatively correlated with *ff* (PPAHs: Pearson's r = -0.472, R^2 = 0.223, Fig. 2(b). SPAHs: Pearson's r = -0.167, R^2 = 0.028, Fig. 2(c)), suggesting there is a close link between molecular weight and partitioning dynamics of PPAHs/SPAHs. Low-molecular-weight PAHs favored the presence in water phase, while high-molecular-weight PPAHs exhibited dominance in sediment phase, which is consistent with previous studies [61]. Regarding different molecular structures, the impacts of different substituents in SPAHs were further explored. It was found that the *ff* values of parent Nap were increased after substituting by carbonyl groups (1, 4-NapQ) and nitro groups (2-NNap), making these substituted Nap more inclined to migrate from sediment into water phase, which can be attributed to the high hydrophilicity of carbonyl and nitro groups. However, methyl substitution (2,7-DMNap, 1,6,7-TMNap, and 1,4,6, 7-TMNap) decreased the *ff* values of parent Nap (Fig. 2(d)), and the number of methyl substituents showed a significant negative correlation with *ff* values (Pearson's r = -0.903, R^2 = 0.816, Fig. 2(e)). This is due to the fact that methyl group is a hydrophobic group and the increase in the number of methyl group favors the enrichment of MPAHs into the sediments. While previous studies emphasized molecular weight, physicochemical properties, and sediment TOC as partitioning determinants [57], this work pioneers the identification of substituent structural motifs as critical regulators of phase distribution. These differential partitioning behaviors of PPAHs and SPAHs between water-sediment phases may have different impacts on microbial ecology in water-sediment systems.

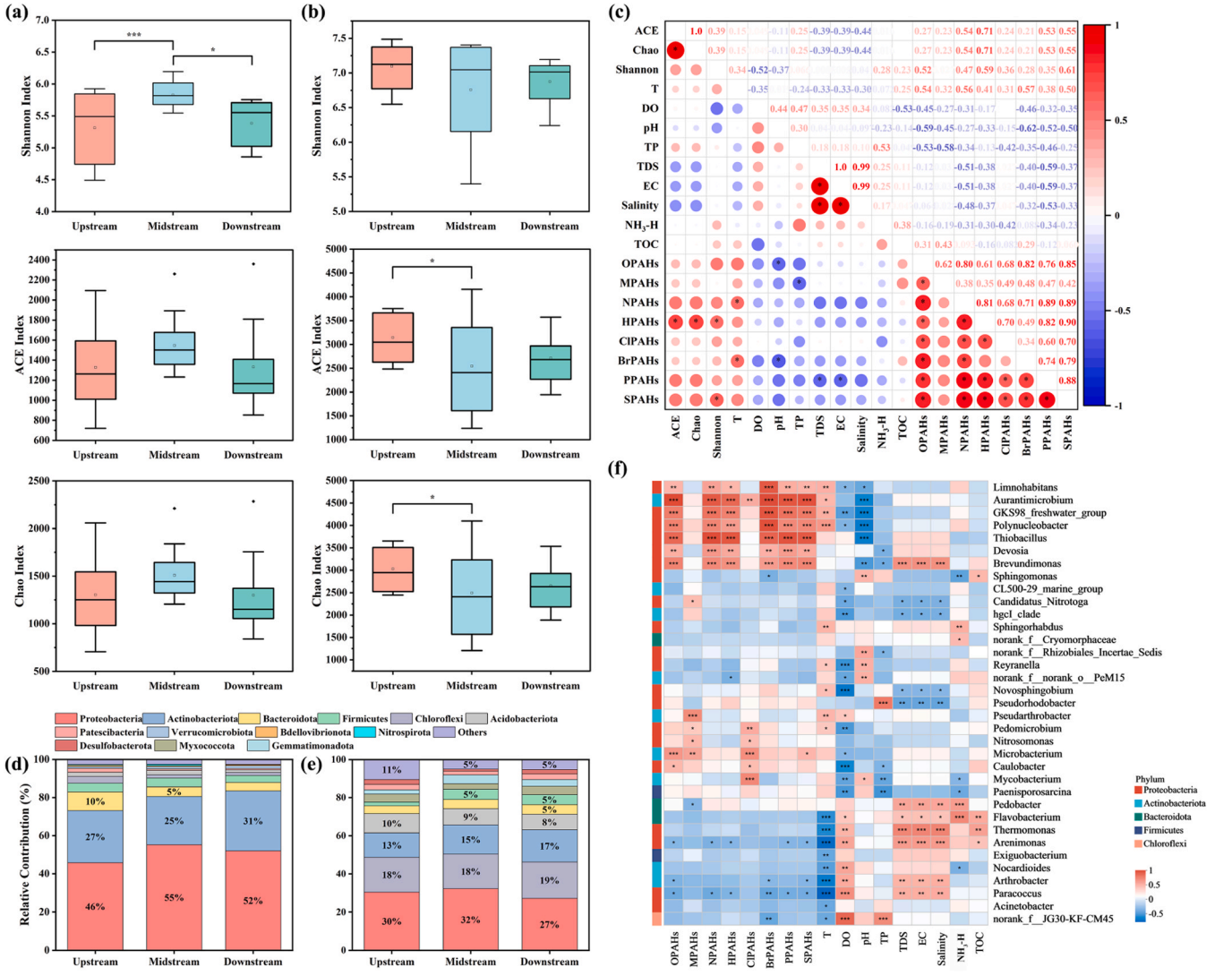

Fig. 3. (a) α-diversity indices (Shannon, ACE, and Chao indices) of microbial community in water phase and (b) sediment phase; (c) Pearson correlation cell plots among α-diversity indices, environmental factors, and concentrations of PPAHs/SPAHs in water phase; (d) microbial community composition at phylum level in water phase and (e) sediment phase (phylum with less than 0.01 % relative abundance in all samples are classified as others); (f) heatmap of PPAHs, SPAHs, environmental factors, and microbial communities of the top 35 species (genus level) in water phase. The significance levels are represented by * ($P < 0.05$), ** ($P < 0.01$), *** ($P < 0.001$).

3.3. PPAH/SPAH inputs induced differential microbial community structures in water and sediment phases

High-throughput sequencing yielded 23,340 and 55,067 amplicon sequence variants (ASVs) from water and sediment phases, respectively, with only 4.8 % (1122) and 3.8 % (2080) shared across upstream-midstream-downstream gradients (Fig. S6), demonstrating PAH-driven divergence in microbial community structures. α-diversity metrics (Shannon, ACE, Chao) revealed phase-dependent responses to coking effluent inputs. Water-phase communities exhibited significantly elevated Shannon indices in midstream area (ANOSIM, $P < 0.01$; Fig. 3 (a)), contrasting with sediment-phase diversity suppression (ANOSIM, $P < 0.05$) (Fig. 3(b)). The same trends in ACE/Chao indices confirmed PAH-mediated trophic divergence, characterized by water-phase enrichment (+16 % mean richness) versus sediment-phase depletion (-18 %) relative to upstream sites before PAH inputs. Pearson correlation cell plots showed that water-phase microbial diversity (indicated by Shannon indices) strongly correlated with SPAH concentrations (R^2=0.61), particularly significantly correlated with HPAH concentrations (R^2=0.59; $P < 0.05$) (Fig. 3(c)). Conversely, sediment-phase microbial diversity displayed a primary association with total organic carbon (TOC, R^2=0.20) followed by PPAHs (R^2=0.17) (Fig. S7), indicating phase-specific selection pressures—aqueous systems favoring SPAH-adapted heterotrophs, while sediment system experienced PPAH-induced oligotrophization.

Furthermore, NMDS ordination based on Bray-Curtis dissimilarity confirmed significant biogeographic divergence among upstream-midstream-downstream microbial assemblages ($P = 0.001$; Fig. S8), validating the spatial grouping rationality. Phylum-level analysis revealed *Proteobacteria* and *Actinobacteriota* collectively constituted 73.12 % of water-phase communities (Fig. 3(d)), while sediment phases were predominated by *Proteobacteria*, *Chloroflexi*, *Actinobacteriota*, and *Acidobacteriota* (71.54 %) (Fig. 3(e)). Redundancy analysis (RDA) identified Temperature ($R^2 = 0.71$, $P = 0.001$), NH_3-H ($R^2 = 0.46$, $P = 0.001$), and MPAHs ($R^2 = 0.32$, $P = 0.003$) as primary water-phase microbial community distribution drivers (Table S10). Notably, SPAHs ($R^2 = 0.17$) exerted stronger microbial compositional control than PPAHs ($R^2 = 0.15$), particularly BrPAHs ($R^2 = 0.23$) and OPAHs ($R^2 = 0.22$). Correlation heatmaps demonstrated significant positive associations ($P < 0.05$) between SPAHs and *Brevundimonas* ($R^2 = 0.63$), *Aurantimicrobium* ($R^2 = 0.85$), and *Thiobacillus* ($R^2 = 0.81$) (Fig. 3(f)). Contrastingly, sediment microbial community distribution was principally governed by TOC ($R^2 = 0.38$), PPAHs ($R^2 = 0.17$), and ClPAHs ($R^2 = 0.16$) (Table S10). PPAHs showed positive correlations with *AKYG1722* ($R^2 = 0.39$) but negative associations with *Gemmatimonadaceae* ($R^2 = -0.32$) and *Haliangium* ($R^2 = -0.38$; Fig. S9). This indicates microbial taxa associated with SPAHs in water phase exhibited marked divergence from those linked to PPAHs in sediment phase, demonstrating phase-specific ecological niche partitioning driven by contaminant physicochemical properties. SPAHs were endowed with polar substituents, compared with hydrophobic PPAHs without functional groups. These findings mechanistically link phase-specific PAH partitioning to divergent microbial selection: SPAHs drive aqueous-phase community restructuring through polar substituent-mediated interactions, while hydrophobic PPAHs preferentially modulate sedimentary assemblages via sorptive enrichment.

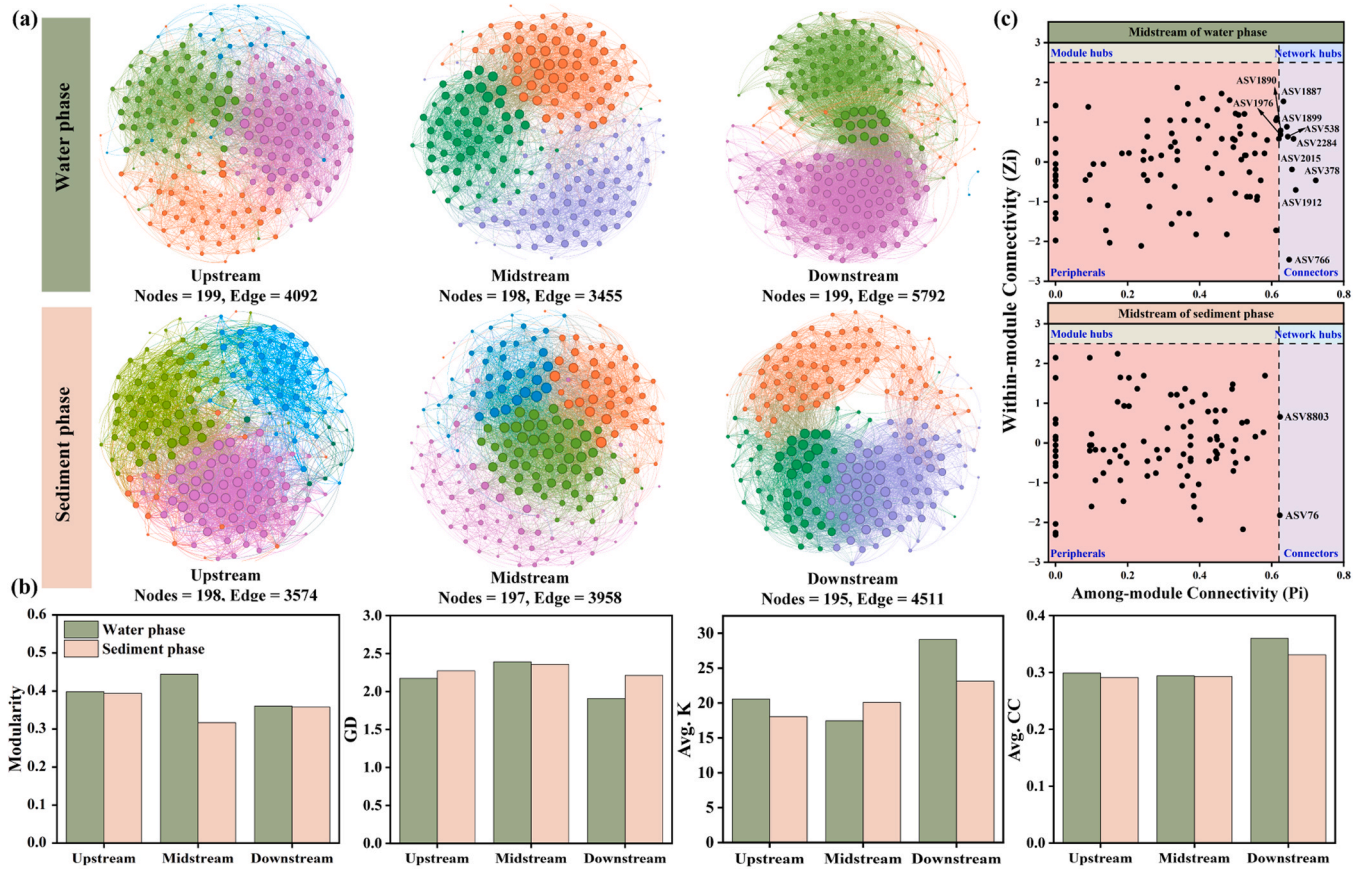

Fig. 4. (a) Microbial co-occurrence networks in water and sediment phase of the receiving river. An edge (connection) between nodes indicates a strong and significant correlation between the two nodes. The size of each node is proportional to the number of connections (degree). The nodes are colored according to the module assigned; (b) topological properties of the microbial co-occurrence networks in water and sediment phase; (c) Pi-Zi plots for bacterial communities in water and sediment phase are displayed based on their topological roles. Each dot denotes an ASV. Distribution of ASVs at module hubs, network hubs, and connectors are considered as keystone species.

3.4. PPAHs/SPAHs inputs shaped different microbial co-occurrence networks and potential keystone species in water and sediment phases

Co-occurrence network analysis elucidated phase-specific microbial interaction dynamics shaped by PPAHs/SPAHs inputs, with ASV-based topological features revealing distinct ecological connectivity patterns across water and sediment phases (Fig. 4). The water-phase midstream network exhibited a 15.6 % reduction in edge count relative to upstream counterparts (Fig. 4(a)), accompanied by decreased average degree (20.56 → 17.45) and clustering coefficient (0.299 → 0.294), alongside increased modularity (0.40 → 0.44) and average path distance (2.17 → 2.39). These topological shifts indicate enhanced niche partitioning and network stability in SPAH-impacted aqueous systems. Conversely, sediment-phase networks demonstrated opposing trends. The modularity declined from 0.394 to 0.317 midstream, while average degree increased (18.05 → 20.09) (Fig. 4(b), Table S11), indicating PPAH-induced disintegration of microbial associations and reduced community stability. This topological differentiation between the water and sediment phases may be related to the evolution of different key species in the network [36].

Thus, keystone species were further identified through network analysis across water-sediment matrices based on centrality and connectivity approach [35]. In midstream water-phase networks, 14 keystone ASVs were found (Fig. 4(c), Table S12). Eight of them were identified to be PAH-degrading taxa, including *Acinetobacter* (ASV4452) [11], *Novosphingobium* (ASV12112) [20], *Devosia* (ASV1887) [7], *Pedobacter* (ASV1976) [1], *Rhodobacter* (ASV538) [37], *Brevundimonas* (ASV2284) [56], *Flavihumibacter* (ASV2015) [1], and *Thermomonas* (ASV378) [46]. The other six keystone ASVs mediated biogeochemical cycling processes, such as sulfur metabolism (*Thiobacillus* (ASV11232) [39], nitrogen fixation (*Rhizobiales Incertae Sedis* (ASV1899) [18], humus degradation (*GKS98_freshwater_group* (ASV4541) [62]), and denitrification (*Devosiaceae* (ASV1890) [52]). Significant positive correlations (R^2 = 0.47–0.81, $P < 0.001$) between SPAHs and keystone genera (*Thiobacillus*, *GKS98_freshwater_group*, *Devosia*, *Brevundimonas*; Fig. 3(f)) suggest SPAHs enrichment promotes functional specialization

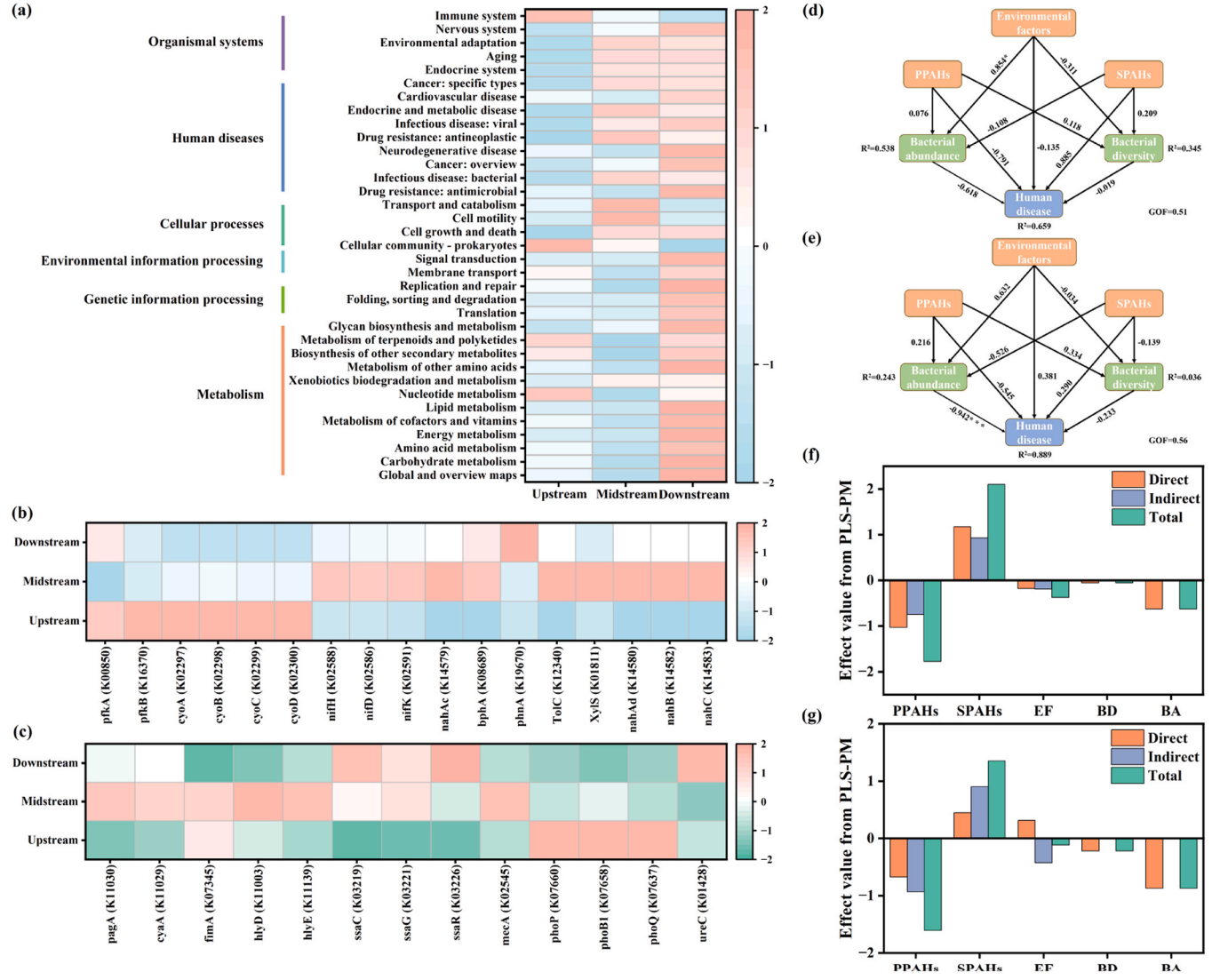

Fig. 5. (a) PICRUSt2 analysis of the ratio of the relative abundance of each functional gene (level-2 metabolic categories) in water phase. Relative functional abundance of (b) metabolism-related genes and (c) pathogenicity-related genes in water phase. The heatmap showed the normalized relative abundance after being centered and scaled in row ("centered" is the process of subtracting the mean of this data to obtain a dataset with a mean of zero; "scaled" is scaling data to a certain range ([-2,2] in our case)). Partial least-squares path model (PLS-PM) revealing the effect degree of environmental factors, PPAHs, SPAHs, bacterial abundance, and bacterial diversity on human disease in (d) water phase and (e) sediment phase. The significance levels are represented by * ($P < 0.05$), ** ($P < 0.01$), *** ($P < 0.001$). Direct and indirect effect values in (f) water phase and (g) sediment phase from PLS-PM. EF: environmental factors; BA: bacterial abundance, BD: bacterial diversity.

in biodegradation and nutrient cycling. Sediment-phase networks yielded five keystone ASVs (Fig. 4(c), Table S12), four exhibiting PAH-degradation capabilities, including *Haliangium* (ASV315) [3], *Sandaracinaceae* (ASV15546) [14], *Bacillus* (ASV8803) [2], and *Phenylobacterium* (ASV76) [44]. The fifth keystone *Subgroup_7* (ASV107) was related to carbohydrate metabolism [19]. In addition, PPAH concentrations positively correlated with *Bacillus* ($R^2 = 0.04$) and *Subgroup_7* ($R^2 = 0.17$; Fig. S9), indicating PPAHs enrichment promotes functional specialization in biodegradation and metabolism. These findings indicate SPAHs enrich water-phase specialists driving coupled PAHs degradation and biogeochemical cycling, while the enrichment of PPAHs in sediments can provide energy support for microbial pairs in oligotrophic environments.

3.5. SPAHs pressure inhibited energy metabolism and promoted pollutant catabolism, while inducing aquatic pathogenicity amplification

Microbial functional analysis via Kyoto Encyclopedia of Genes and Genomes (KEGG) orthology revealed phase-specific metabolic reprogramming in microbial communities. In water phase, metabolism constituted the predominant primary pathway, which exhibited a 2.48 % reduction from upstream to midstream areas (Fig. 5(a), Table S13). Detailed metabolic gene profiling identified suppression of ATP-generating pathways: phosphofructokinase genes (*pfkA* [K00850], *pfkB* [K16370]) critical for glycolysis decreased by 17.8–18.4 %, accompanied by 30.5–31.0 % reductions in cytochrome oxidase subunits (*cyoA-D* [K02297-K02300]) (Fig. 5(b)). This energy metabolism inhibition suggests SPAH-induced oxidative stress, redirecting cellular resources from growth to detoxification processes. KEGG annotation results suggested that these functional shifts were orchestrated through a coordinated molecular network, likely initiated by SPAH-induced oxidative stress. The upregulation of pathways such as MAPK signaling pathway (map04010) and ABC transporters (map02010) indicated a global defensive response to cellular damage (Fig. S10). The observed suppression of glycolysis (map00010) and oxidative phosphorylation (map00190) genes (e.g., *pfkA*, *pfkB*, *cyoA-D*) reflected a strategic "energy-saving mode", reallocating resources from growth to high-cost detoxification processes. Concurrently, the specific activation of PAH-degradation pathways (*nahAc* [K14579], *bphA* [K08689], *phnAxw* [K19670]; +1.1–85.8-fold) and their coupling with glutathione metabolism (map00480) represented a direct metabolic adaptation for detoxification. Crucially, the enrichment of virulence factors might be co-selected through this stress response, as pathways like quorum sensing (map02024) and bacterial secretion systems (map03070) were often under the control of global regulators (e.g., RpoS) that also respond to oxidative stress. This suggests that the upregulation of both degradation and virulence genes is a coordinated survival strategy under severe chemical pressure. Contrastingly, midstream communities exhibited upregulated nitrogen fixation (*nifH* [K02588], *nifD* [K02586], *nifK* [K02591]; +26.6–55.8 %). These functional shifts align with keystone taxa identification (Section 3.4), demonstrating SPAH enrichment selects for dual-function specialists capable of coupled contaminant degradation and nutrient cycling—a strategic adaptation to chemical stress. This metabolic equilibrium between reduced energy production and enhanced biodegradation capacity demonstrates ecological optimization under pollutant pressure. Microbial communities prioritize resource allocation to SPAH catabolism and nitrogen acquisition over growth-associated energetics, enhancing ecosystem resilience through functional redundancy while maintaining structural diversity. Sediment-phase microbial communities exhibited functional attenuation across all six primary metabolic pathways, with organismal systems demonstrating the most pronounced decline from upstream to midstream (-2.88 %; Table S13, Fig. S11). Since PPAHs were the key factors to shape microbial community in sediment phases, these results indicate PPAHs exposure could suppress genetic/environmental information processing, cellular processes, and human disease-associated pathways in benthic microbiomes. Certainly, the potential contributions of other environmental factors—such as hypoxia and nutrient status—should not be overlooked. The relatively stable sedimentary environment conferred greater contaminant resilience compared to water-phase counterparts, resulting in moderated functional shifts.

Notably, pathogenicity-associated pathways exhibited the most pronounced functional enrichment in water-phase microbial communities along the pollution gradient, with a 9.7 % elevation from upstream to midstream areas ($P < 0.001$). Mechanistically, virulence factor analysis revealed significant upregulation of genetic determinants encoding anthrax toxin synthesis (*pagA* [K11030], *cyaA* [K11029]), enterobacterial adhesion (*fimA* [K07345]), extracellular matrix degradation (*hlyD* [K11003], *hlyE* [K11139]), Salmonella Type III secretion systems (*ssaC* [K03219], *ssaG* [K03221], *ssaR* [K03226]), and Staphylococcal methicillin-resistance (*mecA* [K02545]) (Fig. 5(c)). These findings indicate SPAHs' inputs in receiving river exert xenobiotic-mediated virulence selection pressure, stimulating transcriptional activation of pathogenic operons and dissemination of anthropogenic pathogenicity.

Previous studies on microbial functional shifts under pollutant-stressed environments mainly focused on metabolism and information processing [50]. This work emphasized the identification of SPAH-induced aquatic pathogenicity amplification. To further confirm this point, the distributional characteristics and the status of the pathogenic bacteria were analyzed in a targeted manner based on the Human HPB database. Results evidenced that 80 % of top-10 water-phase pathogenic ASVs in midstream areas showed significantly elevated abundances compared with upstream areas ($P < 0.001$), including *Burkholderia* (ASV3452, +42.1-fold), *Corynebacterium* (ASV3442, +17.4-fold), and *Burkholderiales* (ASV3438, +5.7-fold) (Table S14). These taxa represented globally prevalent pathogens associated with melioidosis, diphtheria, and pertussis [4,40,53]. Paradoxically, *Burkholderia* and *Corynebacterium* were also reported to be PAH degraders [60,8], suggesting SPAHs impose dual selection pressures favoring pathogenicity enhancement and metabolic adaptation (PAH degradation capacity). This simultaneous stimulation of pathogenic potential and bioremediation capacity represents an eco-evolutionary dilemma, which underscores the complexity of anthropogenic impacts on aquatic microbiomes. The core mechanism lies in the fact that the high bioavailability and significant toxicity of SPAHs jointly create a strongly selective environment, preferentially enriching multifunctional microbial groups (such as *Burkholderia* and *Corynebacterium*) that possess both PAH-degradation capabilities and inherent pathogenic potential. To counter SPAH-induced oxidative stress, these groups simultaneously upregulate PAH-degradation genes (e.g., *nahAc*, *bphA*) and virulence factor genes (e.g., *mecA*, *pagA*). The latter genes are not merely part of the stress response but evolve as competitive strategies to enhance ecological niche occupation under harsh conditions. Our results mandate integrated assessment models that reconcile contaminant degradation benefits with emergent pathogenicity risks in industrialized watersheds.

To investigate the driving mechanisms of pathogenicity propagation, structural equation modeling (SEM) was employed to deconvolute direct and indirect effects of PPAHs/SPAHs speciation, environmental parameters, and microbial ecology on pathogenic gene abundance. The SEM demonstrated robust explanatory power, accounting for 65.9 % (water phase) and 88.9 % (sediment phase) of variance in human pathogenicity gene distribution (Fig. 5(d-e)). Path analysis showed that SPAHs exhibited strong positive path coefficients ($\beta = 0.885$ [water]; $\beta = 0.290$ [sediment]), whereas PPAHs showed inhibitory relationships ($\beta = -0.791$ [water]; $\beta = -0.545$ (sediment)) (Fig. 5(f-g)). These results further confirm the major roles of SPAHs and PPAHs for determining the microbial function of human pathogenicity in water and sediment phases, respectively. This dual regulation paradigm of water-phase virulence potentiation versus sediment-phase pathogenic suppression establishes SPAHs as critical determinants of aquatic microbiome

pathogenicity, necessitating compound-specific risk assessment frameworks for industrial riverine ecosystems.

3.6. Limitation

This study provides a valuable snapshot of the partitioning behavior of PAHs in the water-sediment system using a fugacity model. However, several limitations should be considered when interpreting our results. Firstly, as noted earlier, our reliance on a single sampling campaign limits our ability to capture seasonal or long-term temporal dynamics influenced by factors such as temperature, hydrological conditions, and microbial activity. Secondly, and equally important, are the inherent simplifications of the fugacity model itself. The equilibrium-based fugacity model does not explicitly account for kinetic processes such as diffusion rates across the sediment-water interface or biological-mediated transport (e.g., bioturbation). Benthic organisms can actively resuspend sediment particles and irrigate porewater, thereby enhancing the exchange of pollutants between solid and aqueous phases and potentially accelerating the attainment of equilibrium or creating non-equilibrium conditions. Our model, by operating on the principle of equilibrium partitioning, may oversimplify these complex, time-dependent interfacial processes. Consequently, the model's outputs represent a simplified estimation of the system's state, potentially overlooking the nuances introduced by biological and physical dynamics at the micro-scale. Despite these limitations, the current model successfully provides a baseline assessment of the equilibrium state towards which the system tends, and effectively identifies the primary partitioning drivers (e.g., organic carbon content, hydrophobicity) under the investigated conditions.

4. Conclusion

This study systematically deciphered the phase-specific environmental behavior and microbiome perturbations induced by PPAHs and SPAHs in a coking-impacted riverine ecosystem, with an emphasis on dissemination of anthropogenic pathogenicity. Three principal findings emerge:

(1) There were significant impacts of coking activity on the receiving river ecosystem. ΣPAHs of water and sediment phases in midstream area exceeded those in the upstream area by a factor of 9.9 and 4.3-fold, respectively. OPAHs (e.g., 9,10-PheQ) dominated water samples (relative contribution: 58.8 %), while PPAHs (e.g., Fla, B[*b*]F, Phe) prevailed in sediments (relative contribution: 72.5 %). Ecological risk was potentially higher in sediment phase than in water phase, with 87.2 % of the RQ values in sediment phase exceeding the risk threshold (RQ >1), while the exceeding rate in water phase was only 50.0 %.

(2) Fugacity fractions showed different partitioning dynamics of PPAHs and SPAHs in water and sediment phases. Polar SPAHs (e.g., OPAHs and NPAHs) demonstrated water-phase enrichment (ff_{mean} = 0.86–0.94) driven by carbonyl/nitro group-mediated hydrophilicity, whereas hydrophobic PPAHs showed sedimentary sequestration (ff_{mean} = 0.65). This led to the predominance of SPAHs in water and PPAHs in sediment phase.

(3) The different partitioning behaviors of PPAHs and SPAHs drove different responses in microbial community in water and sediment phases. SPAHs triggered water-phase functional specialization, elevating α-diversity (+16 %), PAH degradation (*bphA* +85.8-fold), and virulence factor genes (*mecA* +69-fold), while selecting pathogen-degrader hybrids (*Burkholderia-Corynebacterium* consortia). Conversely, PPAHs reduced the α-diversity of microbial communities and inhibited genetic/environmental information processing, cellular processes, and human disease-related pathways in benthic microbiota.

Critically, SPAHs pressure inhibited energy metabolism, promoted pollutant catabolism, while induced dissemination of anthropogenic pathogenicity. They stimulated the proliferation of human pathogens (*Burkholderia*, *Burkholderiales*, and *Corynebacterium*) and amplified the abundance of genes associated with human disease (e.g., *pagA*, *cyaA*, *fimA*, and *mecA*), highlighting an under-recognized health risk. These findings establish a mechanistic framework for understanding contaminant phase partitioning-mediated microbial function shifts, offering critical insights for environmental risk mitigation and public health protection.

Environmental implication

PAHs and their derivatives pose significant threats to riverine ecosystems. Yet, the dynamics of their partitioning in water-sediment systems and the subsequent impacts on river microbial communities remain poorly understood. This study examined the distribution patterns, partitioning behaviors, and microbial responses of PAHs and their derivatives in the water-sediment systems of a coking-polluted receiving river. Pathogenic risks in riverine ecosystems were enhanced due to industrial PAH emissions. The findings construct a mechanistic framework for deciphering how contaminant phase partitioning drives shifts in microbial functions, thereby providing crucial insights for mitigating environmental risks and safeguarding public health.

CRediT authorship contribution statement

Yi Zhong: Visualization, Investigation. **Fan Wang:** Validation, Methodology. **Jukun Xiong:** Validation, Formal analysis. **Wanjun Wang:** Writing – review & editing, Supervision, Project administration, Funding acquisition, Conceptualization. **Chao Wang:** Writing – original draft, Investigation, Formal analysis, Data curation. **Jialin Shi:** Resources, Methodology. **Jiana Zhao:** Software, Formal analysis.

Declaration of Competing interest

The authors declare that they have no known competing financial interests or personal relationships that could have appeared to influence the work reported in this paper.

Acknowledgements

This work was supported by National Natural Science Foundation of China (42377365, 42122056), Guangdong Basic and Applied Basic Research Foundation (2021B1515020063, 2022A1515010815), and National Key Research and Development Program of China (2021YFC1808901).

Appendix A. Supporting information

Supplementary data associated with this article can be found in the online version at doi:10.1016/j.jhazmat.2025.140221.

Data Availability

Data will be made available on request.

References

[1] Ahmad, M., Wang, P.D., Li, J.L., Wang, R.F., Duan, L., Luo, X.Q., Irfan, M., Peng, Z. P., Yin, L.Z., Li, W.J., 2021. Impacts of bio-stimulants on pyrene degradation, prokaryotic community compositions, and functions. Environ Pollut 289, 117863. https://doi.org/10.1016/j.envpol.2021.117863.

[2] Ali, M., Wang, Q., Zhang, Z.X., Chen, X., Ma, M., Tang, Z.W., Li, R., Tang, B., Li, Z. Y., Huang, X.F., Song, X., 2024. Mechanisms of benzene and benzo[a]pyrene biodegradation in the individually and mixed contaminated soils. Environ Pollut 347, 123710. https://doi.org/10.1016/j.envpol.2024.123710.

[3] Badmadashiev, D.V., Stroeva, A.R., Klyukina, A.A., Poludetkina, E.N., Bonch-Osmolovskaya, E.A., 2023. Stratification of prokaryotic communities in the White sea bottom sediments. Microbiology 92, 83–87. https://doi.org/10.1134/S002626172360369X.

[4] Bridel, S., Bouchez, V., Brancotte, B., Hauck, S., Armatys, N., Landier, A., Muhle, E., Guillot, S., Toubiana, J., Maiden, M.C.J., Jolley, K.A., Brisse, S., 2022.

A comprehensive resource for bordetella genomic epidemiology and biodiversity studies. Nat Commun 13, 3807. https://doi.org/10.1038/s41467-022-31517-8.
[5] Burnet, J.B., Demeter, K., Dorner, S., Farnleitner, A.H., Hammes, F., Pinto, A.J., Prest, E.I., Prevost, M., Stott, R., van Bel, N., 2025. Automation of on-site microbial water quality monitoring from source to tap: challenges and perspectives. Water Res 274, 123121. https://doi.org/10.1016/j.watres.2025.123121.
[6] Chen, C.T., Lin, T., Sun, X., Wu, Z.L., Tang, J.H., 2023. Spatiotemporal distribution and particle–water partitioning of polycyclic aromatic hydrocarbons in bohai sea, China. Water Res 244, 120440. https://doi.org/10.1016/j.watres.2023.120440.
[7] Chen, R., Zhao, Z.H., Xu, T., Jia, X.Q., 2023. Microbial consortium HJ-SH with very high degradation efficiency of phenanthrene. Microorganisms 11, 2383. https://doi.org/10.3390/microorganisms11102383.
[8] Chikere, C.B., Chikere, B.O., Okpokwasili, G.C., 2012. Bioreactor-based bioremediation of hydrocarbon-polluted Niger delta marine sediment, Nigeria. 3 Biotech 2, 53–66. https://doi.org/10.1007/s13205-011-0030-8.
[9] Cooke, C.A., Emmerton, C.A., Yi, Y., Levesque, L., Glozier, N., 2022. Polycyclic aromatic compounds in rivers dominated by petrogenic sources after a boreal megafire. Environ Sci Technol 56, 9408–9416. https://doi.org/10.1021/acs.est.2c01671.
[10] Cui, M.K., Xu, S.L., Song, W.Q., Ye, H.B., Huang, J.L., Liu, B.H., Dong, B., Xu, Z.X., 2022. Trace metals, polycyclic aromatic hydrocarbons and polychlorinated biphenyls in the surface sediments from sanya river, China: distribution, sources and ecological risk. Environ Pollut 294, 118614. https://doi.org/10.1016/j.envpol.2021.118614.
[11] Czarny, J., Staninska-Pieta, J., Piotrowska-Cyplik, A., Juzwa, W., Wolniewicz, A., Marecik, R., Lawniczak, L., Chrzanowski, L., 2020. Acinetobacter sp. As the key player in diesel oil degrading community exposed to PAHs and heavy metals. J Hazard Mater 383, 121168. https://doi.org/10.1016/j.jhazmat.2019.121168.
[12] Gong, X.H., Zhao, Z.H., Zhang, L., Yao, S.C., Xue, B., 2022. North-south geographic heterogeneity and control strategies for polycyclic aromatic hydrocarbons (PAHs) in Chinese lake sediments illustrated by forward and backward source apportionments. J Hazard Mater 431, 128545. https://doi.org/10.1016/j.jhazmat.2022.128545.
[13] Guigue, C., Tedetti, M., Dang, D.H., Mullot, J.U., Garnier, C., Goutx, M., 2017. Remobilization of polycyclic aromatic hydrocarbons and organic matter in seawater during sediment resuspension experiments from a polluted coastal environment: insights from toulon bay (France). Environ Pollut 229, 627–638. https://doi.org/10.1016/j.envpol.2017.06.090.
[14] Guo, M.X., Shang, X.T., Ma, Y.L., Zhang, K., Zhang, L., Zhou, Y.M., Gong, Z.Q., Miao, R.H., 2024. Biochars assisted phytoremediation of polycyclic aromatic hydrocarbons contaminated agricultural soil: dynamic responses of functional genes and microbial community. Environ Pollut 345, 123476. https://doi.org/10.1016/j.envpol.2024.123476.
[15] He, W., Yang, C., Liu, W.X., He, Q.S., Wang, Q.M., Li, Y.L., Kong, X.Z., Lan, X.Y., Xu, F.L., 2016. The partitioning behavior of persistent toxicant organic contaminants in eutrophic sediments: coefficients and effects of fluorescent organic matter and particle size. Environ Pollut 219, 724–734. https://doi.org/10.1016/j.envpol.2016.07.014.
[16] Hong, W.J., Jia, H.L., Li, Y.F., Sun, Y., Liu, X.J., Wang, L., 2016. Polycyclic aromatic hydrocarbons (PAHs) and alkylated PAHs in the coastal seawater, surface sediment and oyster from dalian, northeast China. Ecotoxicol Environ Saf 128, 11–20. https://doi.org/10.1016/j.ecoenv.2016.02.003.
[17] Idowu, O., Tran, T.K.A., Baker, P., Farrel, H., Zammit, A., Semple, K.T., O'Connor, W., Thavamani, P., 2020. Bioavailability of polycyclic aromatic compounds (PACs) to the Sydney rock oyster (Saccostrea glomerata) from sediment matrices of an economically important Australian estuary. Sci Total Environ 736, 139574. https://doi.org/10.1016/j.scitotenv.2020.139574.
[18] Jia, L.P., Jiang, B.H., Huang, F., Hu, X.M., 2019. Nitrogen removal mechanism and microbial community changes of bioaugmentation subsurface wastewater infiltration system. Bioresour Technol 294, 122140. https://doi.org/10.1016/j.biortech.2019.122140.
[19] Kuo, J., Liu, D., Wen, W.H., Chiu, C.Y., Chen, W., Wu, Y.W., Lai, F.T., Lin, C.H., 2024. Different microbial communities in paddy soils under organic and nonorganic farming. Braz J Microbiol 55, 777–788. https://doi.org/10.1007/s42770-023-01218-5.
[20] Laothamteep, N., Kawano, H., Vejarano, F., Suzuki-Minakuchi, C., Shintani, M., Nojiri, H., Pinyakong, O., 2021. Effects of environmental factors and coexisting substrates on PAH degradation and transcriptomic responses of the defined bacterial consortium OPK. Environ Pollut 277, 116769. https://doi.org/10.1016/j.envpol.2021.116769.
[21] Li, R.F., Luo, Y., Zhu, X., Zhang, J., Wang, Z.Y., Yang, W., Li, Y., Li, H., 2024. Anthropogenic impacts on polycyclic aromatic hydrocarbons in surface water: evidence from the COVID-19 lockdown. Water Res 262, 122143. https://doi.org/10.1016/j.watres.2024.122143.
[22] Li, X.Y., Li, T., Wang, F.S., Chen, X.P., Qin, Y., Chu, Y.S., Yang, M., Zhang, Z.F., Ma, J., 2024. Distribution and sources of polycyclic aromatic hydrocarbons in cascade reservoir sediments: influence of anthropogenic activities and reservoir hydrology. Environ Geochem Health 46, 487. https://doi.org/10.1007/s10653-024-02256-0.
[23] Lima, A.L.C., Farrington, J.W., Reddy, C.M., 2005. Combustion-Derived polycyclic aromatic hydrocarbons in the Environment—A review. Environ Forensics 6, 109–131. https://doi.org/10.1080/15275920590952739.
[24] Lin, W., Fan, F.Q., Xu, G.M., Gong, K.Y., Cheng, X., Yuan, X.Y., Zhang, C., Gao, Y., Wang, S.R., Ng, H.Y., Dong, Y., 2023. Microbial community assembly responses to polycyclic aromatic hydrocarbon contamination across water and sediment habitats in the pearl river estuary. J Hazard Mater 457, 131762. https://doi.org/10.1016/j.jhazmat.2023.131762.
[25] Liu, C.Y., Huang, Z.F., Qadeer, A., Liu, Y., Qiao, X.C., Zheng, B.H., Zhao, G.F., Zhao, X.R., 2021. The sediment-water diffusion and risk assessment of PAHs in different types of drinking water sources in the Yangtze river delta, China. J Clean Prod 309, 127456. https://doi.org/10.1016/j.jclepro.2021.127456.
[26] Liu, J.B., Zhang, C., Jia, H.Z., Lichtfouse, E., Sharma, V.K., 2022. Abiotic transformation of polycyclic aromatic hydrocarbons via interaction with soil components: a systematic review. CRIT REV ENV SCI TEC 53, 676–699. https://doi.org/10.1080/10643389.2022.2083897.
[27] Liu, Y., Beckingham, B., Ruegner, H., Li, Z., Ma, L.M., Schwientek, M., Xie, H., Zhao, J.F., Grathwohl, P., 2013. Comparison of sedimentary PAHs in the rivers of ammer (Germany) and liangtan (China): differences between Early- and Newly-Industrialized countries. Environ Sci Technol 47, 701–709. https://doi.org/10.1021/es3031566.
[28] Liu, Y., He, Y., Han, B.J., Liu, H.J., Tao, S., Liu, W.X., 2023. Sewage discharge and organic matter affect the partitioning behaviors of different polycyclic aromatic hydrocarbons in a river surface sediment-pore water system. J Hazard Mater 446, 130757. https://doi.org/10.1016/j.jhazmat.2023.130757.
[29] Liu, Y., He, Y., Liu, Y., Liu, H.J., Tao, S., Liu, W.X., 2023. Source identification and ecological risks of parent and substituted polycyclic aromatic hydrocarbons in river surface sediment-pore water systems: effects of multiple factors. Sci Total Environ 858, 159921. https://doi.org/10.1016/j.scitotenv.2022.159921.
[30] Liu, Y., Huang, Y.H., Lu, H.X., Li, H., Li, Y.W., Mo, C.H., Cai, Q.Y., 2021. Persistent contamination of polycyclic aromatic hydrocarbons (PAHs) and phthalates linked to the shift of microbial function in urban river sediments. J Hazard Mater 414, 125416. https://doi.org/10.1016/j.jhazmat.2021.125416.
[31] Liu, Y.R., van der Heijden, M.G.A., Riedo, J., Sanz-Lazaro, C., Eldridge, D.J., Bastida, F., Moreno-Jimenez, E., Zhou, X.Q., Hu, H.W., He, J.Z., Moreno, J.L., Abades, S., Alfaro, F., Bamigboye, A.R., Berdugo, M., Blanco-Pastor, J.L., de Los Rios, A., Duran, J., Grebenc, T., Illan, J.G., Makhalanyane, T.P., Molina-Montenegro, M.A., Nahberger, T.U., Penaloza-Bojaca, G.F., Plaza, C., Rey, A., Rodriguez, A., Siebe, C., Teixido, A.L., Casado-Coy, N., Trivedi, P., Torres-Diaz, C., Verma, J.P., Mukherjee, A., Zeng, X.M., Wang, L., Wang, J., Zaady, E., Zhou, X., Huang, Q., Tan, W., Zhu, Y.G., Rillig, M.C., Delgado-Baquerizo, M., 2023. Soil contamination in nearby natural areas mirrors that in urban greenspaces worldwide. Nat Commun 14, 1706. https://doi.org/10.1038/s41467-023-37428-6.
[32] Louvado, A., Gomes, N.C.M., Simões, M.M.Q., Almeida, A., Cleary, D.F.R., Cunha, A., 2015. Polycyclic aromatic hydrocarbons in deep sea sediments: Microbe–pollutant interactions in a remote environment. Sci Total Environ 526, 312–328. https://doi.org/10.1016/j.scitotenv.2015.04.048.
[33] Lu, J.X., Li, M.T., Tan, J.C., He, M.Y., Wu, H.M., Kang, Y., Hu, Z., Zhang, J., Guo, Z. Z., 2023. Distribution, sources, ecological risk and microbial response of polycyclic aromatic hydrocarbons in qingdao bays, China. Environ Pollut 338, 122687. https://doi.org/10.1016/j.envpol.2023.122687.
[34] Luo, J., Huang, G.B., Wang, M., Zhang, Y.N., Liu, Z.X., Zhang, Q., Bai, S.Y., Xu, D. D., Liu, H.L., Mo, S.P., Zhou, X.B., Fu, M.M., 2025. Composition characteristics, source analysis and risk assessment of PAHs in surface waters of lipu. J Hazard Mater 490, 137733. https://doi.org/10.1016/j.jhazmat.2025.137733.
[35] Ma, B., Wang, H.Z., Dsouza, M., Lou, J., He, Y., Dai, Z.M., Brookes, P.C., Xu, J.M., Gilbert, J.A., 2016. Geographic patterns of co-occurrence network topological features for soil microbiota at continental scale in eastern China. ISME J 10, 1891–1901. https://doi.org/10.1038/ismej.2015.261.
[36] Mee, M.T., Collins, J.J., Church, G.M., Wang, H.H., 2014. Syntrophic exchange in synthetic microbial communities. Proc Natl Acad Sci USA 111, E2149–E2156. https://doi.org/10.1073/pnas.1405641111.
[37] Meng, S.S., Peng, T., Liu, Y.J., Zhang, S., Qian, Z.H., Huang, T.W., Xie, Q.Y., Gu, J. D., Hu, Z., 2024. Novel insights into the synergetic degradation of pyrene by microbial communities from mangroves in China. J Hazard Mater 469, 133907. https://doi.org/10.1016/j.jhazmat.2024.133907.
[38] Moody, J.D., Freeman, J.P., Doerge, D.R., Cerniglia, C.E., 2001. Degradation of phenanthrene and anthracene by cell suspensions of mycobacterium sp. Strain PYR-1. Appl Environ Microbiol 67, 1476–1483. https://doi.org/10.1128/AEM.67.4.1476-1483.2001.
[39] O'Brien, L., Siboni, N., Seymour, J.R., Balzer, M., Mitrovic, S., 2023. Tributary inflows to a regulated river influence bacterial communities and increase bacterial carbon assimilation. Microb Ecol 86, 2642–2654. https://doi.org/10.1007/s00248-023-02271-1.
[40] Petras, J.K., Elrod, M.G., Ty, M.C., Dawson, P., O'Laughlin, K., Gee, J.E., Hanson, J., Boutwell, C., Ainsworth, G., Beesley, C.A., Saile, E., Tiller, R., Gulvik, C. A., Ware, D., Sokol, T., Balsamo, G., Taylor, K., Salzer, J.S., Bower, W.A., Weiner, Z.P., Negron, M.E., Hoffmaster, A.R., Byers, P., 2023. Locally acquired melioidosis linked to environment - Mississippi, 2020-2023. N Engl J Med 389, 2355–2362. https://doi.org/10.1056/NEJMoa2306448.
[41] Qiao, M., Qi, W.X., Liu, H.J., Qu, J.H., 2014. Occurrence, behavior and removal of typical substituted and parent polycyclic aromatic hydrocarbons in a biological wastewater treatment plant. Water Res 52, 11–19. https://doi.org/10.1016/j.watres.2013.12.032.
[42] Qiao, M., Qi, W.X., Liu, H.J., Qu, J.H., 2022. Oxygenated polycyclic aromatic hydrocarbons in the surface water environment: occurrence, ecotoxicity, and sources. Environ Int 163, 107232. https://doi.org/10.1016/j.envint.2022.107232.
[43] Qiu, L.P., Zhang, Q., Zhu, H.S., Reich, P.B., Banerjee, S., van der Heijden, M.G.A., Sadowsky, M.J., Ishii, S., Jia, X.X., Shao, M.G., Liu, B.Y., Jiao, H., Li, H.Q., Wei, X. R., 2021. Erosion reduces soil microbial diversity, network complexity and multifunctionality. ISME J 15, 2474–2489. https://doi.org/10.1038/s41396-021-00913-1.

[44] Shang, X.T., Wu, S.R., Liu, Y.L., Zhang, K.K., Guo, M.X., Zhou, Y.M., Zhu, J.W., Li, X.H., Miao, R.H., 2024. Rice husk and its derived biochar assist phytoremediation of heavy metals and PAHs co-contaminated soils but differently affect bacterial community. J Hazard Mater 466, 133684. https://doi.org/10.1016/j.jhazmat.2024.133684.

[45] Shao, B., Xie, Y.G., Zhang, L., Ruan, Y., Liang, B., Zhang, R.C., Xu, X.J., Wang, W., Lin, Z.D., Pei, X.Y., Wang, X.T., Zhao, L., Zhou, X., Wu, X.H., Xing, D.F., Wang, A.J., Lee, D.J., Ren, N.Q., Canfield, D.E., Hedlund, B.P., Hua, Z.S., Chen, C., 2025. Versatile nitrate-respiring heterotrophs are previously concealed contributors to sulfur cycle. Nat Commun 16, 1202. https://doi.org/10.1038/s41467-025-56588-1.

[46] Smulek, W., Sydow, M., Zabielska-Matejuk, J., Kaczorek, E., 2020. Bacteria involved in biodegradation of creosote PAH - a case study of long-term contaminated industrial area. Ecotoxicol Environ Saf 187, 109843. https://doi.org/10.1016/j.ecoenv.2019.109843.

[47] Van Metre, P.C., Mahler, B.J., Qi, S.L., Gellis, A.C., Fuller, C.C., Schmidt, T.S., 2022. Sediment sources and Sealed-Pavement area drive polycyclic aromatic hydrocarbon and metal occurrence in urban streams. Environ Sci Technol 56, 1615–1626. https://doi.org/10.1021/acs.est.1c00414.

[48] Wang, C., Wang, W.J., Shao, S.B., Deng, W.Q., Wang, C.Q., Liu, X.Y., Li, H.L., Wen, M.C., Zhang, X., Li, G.Y., An, T.C., 2024. Occurrence of BTX and PAHs in underground drinking water of coking contaminated sites: linkage with altitude and health risk assessment by boiling-modified models. Sci Total Environ 917, 170407. https://doi.org/10.1016/j.scitotenv.2024.170407.

[49] Wang, J., Wang, J., Zhao, Z.L., Chen, J.W., Lu, H., Liu, G.F., Zhou, J.T., Guan, X.Y., 2017. PAHs accelerate the propagation of antibiotic resistance genes in coastal water microbial community. Environ Pollut 231, 1145–1152. https://doi.org/10.1016/j.envpol.2017.07.067.

[50] Wang, S., Wang, J.W., Liu, Z.Q., Zhang, B.G., 2022. Unraveling diverse survival strategies of microorganisms to vanadium stress in aquatic environments. Water Res 221, 118813. https://doi.org/10.1016/j.watres.2022.118813.

[51] Wang, Z.M., Liang, Z.S., Li, G.Y., An, T.C., 2024. Odorous organic gas emission characteristics from cooked food wastes during aerobic decomposition. J Clean Prod 434, 139961. https://doi.org/10.1016/j.jclepro.2023.139961.

[52] Weldmichael, T.G., Márton, D., Simon, B., Michéli, E., Reda, G.T., Adiyah, F., Cserháti, M., 2021. Bacterial community characterization and microbial respiration of selected arable soils of Ethiopia. EURASIAN SOIL SCI 54, 1921–1934. https://doi.org/10.1134/s1064229321120140.

[53] Wittchen, M., Busche, T., Gaspar, A.H., Lee, J.H., Ton-That, H., Kalinowski, J., Tauch, A., 2018. Transcriptome sequencing of the human pathogen corynebacterium diphtheriae NCTC 13129 provides detailed insights into its transcriptional landscape and into DtxR-mediated transcriptional regulation. BMC Genom 19, 82. https://doi.org/10.1186/s12864-018-4481-8.

[54] Xu, N.H., Chen, B.F., Wang, Y., Lei, C.T., Zhang, Z.Y., Ye, Y.Q., Jin, M.K., Zhang, Q., Lu, T., Dong, H.P., Shou, J.X., Penuelas, J., Zhu, Y.G., Qian, H.F., 2024. Integrating Anthropogenic-Pesticide interactions into a soil Health-Microbial index for sustainable agriculture at global scale. Glob Chang Biol 30, e17596. https://doi.org/10.1111/gcb.17596.

[55] Xu, S.S., Liu, W.X., Tao, S., 2006. Emission of polycyclic aromatic hydrocarbons in China. Environ Sci Technol 40, 702–708.

[56] Yuan, J., Lai, Q.L., Sun, F.Q., Zheng, T.L., Shao, Z.Z., 2015. The diversity of PAH-degrading bacteria in a deep-sea water column above the southwest Indian ridge. Front Microbiol 6, 853. https://doi.org/10.3389/fmicb.2015.00853.

[57] Zhang, L.H., Ma, Y.X., Cai, M.H., Zhong, Y.S., Zhang, Z.W., Li, S.Z., 2023. Chemodynamics of polycyclic aromatic hydrocarbons and their alkylated and nitrated derivatives in the yellow sea and east China Sea. Environ Sci Technol 57, 20292–20303. https://doi.org/10.1021/acs.est.3c07476.

[58] Zhang, X., Wang, X.L., Liang, W.G., Liu, M.M., Wang, X., Zhao, X.L., 2024. The occurrence, sources, and health risks of substituted polycyclic aromatic hydrocarbons (SPAHs) cannot be ignored. Environ Int 183, 108390. https://doi.org/10.1016/j.envint.2023.108390.

[59] Zhang, Y.X., Cheng, D.D., Lei, Y.L., Song, J.X., Xia, J., 2022. Spatiotemporal distribution of polycyclic aromatic hydrocarbons in sediments of a typical river located in the loess plateau, China: influence of human activities and land-use changes. J Hazard Mater 424, 127744. https://doi.org/10.1016/j.jhazmat.2021.127744.

[60] Zhao, Z.H., Chen, W., Cheng, Y., Li, J.B., Chen, Z.L., 2023. Burkholderia cepacia immobilized onto rGO as a biomaterial for the removal of naphthalene from wastewater. Environ Res 235, 116663. https://doi.org/10.1016/j.envres.2023.116663.

[61] Zhao, Z.H., Gong, X.H., Zhang, L., Jin, M., Cai, Y.J., Wang, X.L., 2021. Riverine transport and water-sediment exchange of polycyclic aromatic hydrocarbons (PAHs) along the middle-lower Yangtze river, China. J Hazard Mater 403, 123973. https://doi.org/10.1016/j.jhazmat.2020.123973.

[62] Zheng, X., Zhang, W., Wu, Y., Wu, J., Chen, Y.G., Long, M., 2024. Biodegradation of organosulfur with extra carbon source: insights into biofilm formation and bacterial metabolic processes. Sci Total Environ 951, 175758. https://doi.org/10.1016/j.scitotenv.2024.175758.

[63] Zhou, Y.Q., Cheng, L., Lian, Y., Feng, J.Y., Zhou, M.L., Jing, D., Yin, W.W., Wang, H.L., Liu, L., 2024. High-proportions of tailwater discharge alter microbial community composition and assembly in receiving sediments. Sci Rep 14, 14171. https://doi.org/10.1038/s41598-024-63859-2.